

PERTURBATION STABILITY OF COHERENT RIESZ SYSTEMS UNDER CONVOLUTION OPERATORS

WERNER KOZEK¹, GÖTZ PFANDER², AND GEORG ZIMMERMANN^{2,*}

¹Siemens AG

Information and Communication Networks
Hofmannstr. 51, D-81359, Munich, Germany

²Institut f. Angew. Math. & Stat.

Universität Hohenheim, D-70593 Stuttgart, Germany

*(Corresponding author) gzim@uni-hohenheim.de

Tel.: +49 / 711 / 459-2449

Fax.: +49 / 711 / 459-3030

ABSTRACT. We study the orthogonal perturbation of various coherent function systems (Gabor systems, Wilson bases, and wavelets) under convolution operators. This problem is of key relevance in the design of modulation signal sets for digital communication over time-invariant channels. Upper and lower bounds on the orthogonal perturbation are formulated in terms of spectral spread and temporal support of the prototype, and by the approximate design of worst case convolution kernels. Among the considered bases, the Weyl-Heisenberg structure which generates Gabor systems turns out to be optimal whenever the class of convolution operators satisfies typical practical constraints.

1. INTRODUCTION

A coherent function system is built from a finite number of prototype functions by the group action of unitary operators such as translation, modulation and/or scaling. The inherent structure of such systems leads to computationally efficient design and implementation of frames or Riesz bases. The most prominent coherent function systems are wavelet and Gabor systems. Both structures are potential candidates in the two fundamental applications of modern digital communication:

- *Source coding (signal compression)*: The coherent function system conveys the transform step which aims at decorrelating the data prior to quantization. In near-to-lossless compression completeness is a must, hence the function system is required to be a frame.
- *Modulation (signal synthesis)*: The channel input signal is synthesized as a linear combination of certain basis functions whose coefficients are bearing the information. Here, injectivity of this synthesis mapping is crucial, therefore one actually wants to use a Riesz basis for some closed subspace of the underlying Hilbert space (on which the channel acts as a linear operator).

In both applications, the performance is reflected by an operator diagonalization problem; the operator corresponds either to the correlation of the source or to the action of the channel, respectively. Since the a priori knowledge of the underlying operator is incomplete, we are looking for eigenbases which simultaneously diagonalize the class of all possible operators. This is only possible if this operator class is commutative, and even if this is the case, the resulting eigenbases might be unstructured or might not satisfy practical side constraints. The eigenfunctions of convolution operators, for example, are complex exponentials of infinite duration. Nevertheless, when considering convolution

operators whose impulse responses are of finite duration, we can circumvent the problem of infinite duration and achieve exact diagonalization using a *Weyl–Heisenberg* system with *cyclic prefix* (see the remark in Section 3, and Section 4.1).

In this paper, we concentrate on modulation. As transmission bases, we consider shift-invariant Riesz systems $g_{k,l}$ defined by

$$(1.1) \quad g_{k,l}(x) = g_l(x-ak), \quad k \in \mathbb{Z}, \quad l = 0, 1, \dots, N-1,$$

where $a > 0$ is the time shift, each g_l has compact support (fulfilling latency constraints as found in speech communication for example), and the family has one of the following specific structures:

- *Gabor* or *Weyl–Heisenberg* systems [8] correspond to a rectangular tiling of the time–frequency plane, the g_l are modulated versions of a prototype function g_0 :

$$g_l(x) = g_0(x)e^{2\pi i b l x}.$$

Note that in order to have existence of Riesz families, one necessarily has $b \geq 1/a$.

- The real-valued *Wilson* bases [2, 5] have a structure related to but different from the *Weyl–Heisenberg* systems:

$$\begin{aligned} g_0(x) &= g(x), \\ g_m^{(1)}(x) &= g(x) \sqrt{2} \cos(2\pi \frac{2m}{a} x), & g_m^{(2)}(x) &= g(x - \frac{a}{2}) \sqrt{2} \cos(2\pi \frac{2m-1}{a} x), \\ g_m^{(3)}(x) &= g(x) \sqrt{2} \sin(2\pi \frac{2m-1}{a} x), & g_m^{(4)}(x) &= g(x - \frac{a}{2}) \sqrt{2} \sin(2\pi \frac{2m}{a} x), \\ & & m &= 1, \dots, M \quad (\text{i.e., } N = 4M+1). \end{aligned}$$

- The popular dyadic *wavelet* bases [4, 13]:

$$\begin{aligned} g_m^{(n)}(x) &= 2^{m/2} g_0(2^m(x - n \frac{a}{2^m})), \quad m = 0, 1, \dots, M, \quad n = 0, 1, \dots, 2^m - 1 \\ & \quad (\text{i.e., } N = 2^{M+1} - 1). \end{aligned}$$

The transmission signal is given by a doubly-indexed series

$$f(x) = \sum_{k=-\infty}^{\infty} \sum_{l=0}^{N-1} c_{k,l} g_l(x-ak),$$

where $c_{k,l}$ are the information bearing complex-valued coefficients. In digital communication applications these coefficients are elements of a finite alphabet (“QAM Constellation”), but for our purpose it is more appropriate to assume a Hilbert space setting, i.e., $\{c_{k,l}\} \in \ell^2$.

After transmission over a physical communication channel, the received signal can be split up into a linearly transformed version of the transmitted signal and statistically independent additive noise n , so we obtain

$$r(x) = (K f)(x) + n(x).$$

We assume throughout this paper that the channel distortion corresponds to a translation invariant system, i.e.,

$$(K f)(x) = (K_h f)(x) = (h * f)(x) = \int_{\mathbb{R}} h(x-y) f(y) dy$$

for some $h \in \mathbf{L}^2(\mathbb{R}) \cap \mathbf{L}^1(\mathbb{R})$. It should be emphasized, however, that strict translation invariance is always an approximation whose validity has to be checked for the critical time scale in question. In the present context the critical scale is the length of the (finite support) prototype function g_0 which is short enough that K can well be considered as a

convolution operator. Since h and thus K_h are not fixed, but will vary from case to case, we consider the following ensemble of possible impulse responses:

(1.2)

$$\mathcal{H} = \left\{ h \in \mathbf{L}^2(\mathbb{R}) : \text{supp } h \subseteq \left[-\frac{x_0}{2}, +\frac{x_0}{2}\right], \int_{\mathbb{R}} |h(x)|^2 x dx = 0, \|\widehat{h}\|_{\mathbf{L}^\infty} = \sup |\widehat{h}(\xi)| = 1 \right\}.$$

The three conditions imposed on h seem realistic for the following reasons:

- The receiver does not know when the transmission starts, so he has to fix the time $t = 0$ in some way. Since this is equivalent to choosing some translate of h , we may as well fix $|h|^2$ to have vanishing first moment.
- Although h does not have compact support, we may cut it off at some point and treat the influence of the remaining part as noise.
- Consequently, we have $h \in \mathbf{L}^1(\mathbb{R})$, so $\widehat{h} \in \mathbf{L}^\infty(\widehat{\mathbb{R}})$, and we may normalize h in some arbitrary way by assuming an appropriate amplifier.

Outline of the paper. In the following section, we introduce the concept of orthogonal perturbation, and derive upper and lower bounds on this quantity for a given function under a class of channel operators. These bounds are formulated in terms of the spectral variance and the temporal support of the prototype function. The lower bound is obtained by the approximate design of a worst case operator via an interpolation procedure.

In Section 3, we numerically compare the three above-mentioned structures of coherent Riesz bases using these upper and lower bounds. The numerical parameters we use are chosen to be compatible with the digital subscriber loop setup.

Finally, in Section 4, we illustrate the performance of these Riesz bases when perturbed by a realization of a twisted copper cable impulse response. This comparison shows the validity and importance of the theoretical results obtained in Section 2.

Notation. For the Fourier transformation, we use the normalization

$$\widehat{f}(\xi) = \int_{\mathbb{R}} f(x) e^{-2\pi i \xi x} dx \quad \text{for } \xi \in \widehat{\mathbb{R}} = \mathbb{R}.$$

Consequently, we can define the inverse Fourier transformation via

$$\check{g}(x) = \int_{\widehat{\mathbb{R}}} g(\xi) e^{2\pi i \xi x} d\xi$$

to obtain $(\widehat{f})^\vee = f$.

We define the translation operator by

$$(\tau_y f)(x) = f(x-y),$$

it has the property

$$(\tau_\eta \widehat{\varphi})^\vee = e^{2\pi i \eta x} \varphi.$$

For $A \subset \mathbb{R}$ we define the characteristic function of A by

$$\chi_A(x) = \begin{cases} 1 & \text{if } x \in A \\ 0 & \text{if } x \notin A \end{cases}.$$

2. ORTHOGONAL PERTURBATIONS

As mentioned in the introduction, an optimal function system $\{g_{k,l}\}$ would consist of eigenfunctions of K_h . Since this is impossible to achieve for all h of arbitrary support, we aim for approximate eigenfunctions and use the orthogonal perturbation of the g_l by K_h as a measure of stability, i.e.,

$$d_{g,h} = \left\| K_h g - P_{\langle g \rangle}(K_h g) \right\|_{\mathbf{L}^2},$$

where $P_{\langle g \rangle}$ is the orthogonal projection onto the span of g , given by $P_{\langle g \rangle}(K_h g) = \frac{\langle K_h g, g \rangle}{\langle g, g \rangle} g$ (cf., Figure 1).

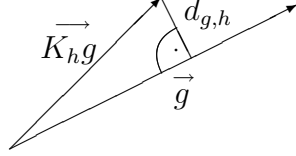


FIGURE 1.

Assuming $\langle g, g \rangle = \|g\|^2 = 1$, we obtain by the Pythagorean theorem

$$(2.1) \quad d_{g,h}^2 = \|K_h g\|^2 - |\langle K_h g, g \rangle|^2.$$

Since the convolution $K_h g = h * g$ corresponds to multiplication in the Fourier domain, $d_{g,h}$ can be related to the frequency localization of g , as the following lemma shows.

Lemma 2.1. *Let $g, h \in \mathbf{L}^2(\mathbb{R})$ with $\|g\|_{\mathbf{L}^2} = 1$. Then*

$$(2.2) \quad d_{g,h}^2 = \mathbb{V} \{ \widehat{h}(\Xi) \},$$

where Ξ is a random variable with probability density $|\widehat{g}|^2$, i.e., the variance \mathbb{V} of $\widehat{h}(\Xi)$ is given by

$$\mathbb{V} \{ \widehat{h}(\Xi) \} = \int_{\widehat{\mathbb{R}}} |\widehat{h}(\xi) - \mathbb{E} \{ \widehat{h}(\Xi) \}|^2 |\widehat{g}(\xi)|^2 d\xi,$$

where \mathbb{E} is the expected value

$$\mathbb{E} \{ \widehat{h}(\Xi) \} = \int_{\widehat{\mathbb{R}}} \widehat{h}(\xi) |\widehat{g}(\xi)|^2 d\xi.$$

Proof.

$$\begin{aligned} d_{g,h}^2 &= \|h * g\|_{\mathbf{L}^2(\mathbb{R})}^2 - |\langle h * g, g \rangle_{\mathbf{L}^2(\mathbb{R})}|^2 \\ &= \|\widehat{h} \cdot \widehat{g}\|_{\mathbf{L}^2(\widehat{\mathbb{R}})}^2 - |\langle \widehat{h} \cdot \widehat{g}, \widehat{g} \rangle_{\mathbf{L}^2(\widehat{\mathbb{R}})}|^2 \\ &= \int_{\widehat{\mathbb{R}}} |\widehat{h}(\xi) \widehat{g}(\xi)|^2 d\xi - \left| \int_{\widehat{\mathbb{R}}} \widehat{h}(\xi) \widehat{g}(\xi) \overline{\widehat{g}(\xi)} d\xi \right|^2 \\ &= \int_{\widehat{\mathbb{R}}} |\widehat{h}(\xi)|^2 |\widehat{g}(\xi)|^2 d\xi - \left| \int_{\widehat{\mathbb{R}}} \widehat{h}(\xi) |\widehat{g}(\xi)|^2 d\xi \right|^2 \\ &= \mathbb{E} \{ |\widehat{h}(\Xi)|^2 \} - |\mathbb{E} \{ \widehat{h}(\Xi) \}|^2 \\ &= \mathbb{E} \{ |\widehat{h}(\Xi) - \mathbb{E} \{ \widehat{h}(\Xi) \}|^2 \}. \end{aligned}$$

□

Upper bound. Using the identity (2.2), we can find an upper bound for the orthogonal perturbation $d_{g,h}$ for all $h \in \mathcal{H}$. For simplicity, we define

$$d_g = \sup_{h \in \mathcal{H}} d_{g,h}.$$

Proposition 2.2. For $g \in \mathbf{L}^2(\mathbb{R})$ with $\|g\|_{\mathbf{L}^2} = 1$, we have

$$d_g^2 \leq (\pi x_0)^2 \sigma_{|\widehat{g}|^2}^2,$$

where $\sigma_{|\widehat{g}|^2}^2$ is the variance of $|\widehat{g}|^2$, i.e.,

$$\sigma_{|\widehat{g}|^2}^2 = \int_{\widehat{\mathbb{R}}} (\xi - \mu)^2 |\widehat{g}(\xi)|^2 d\xi \quad \text{with} \quad \mu = \mu_{|\widehat{g}|^2} = \int_{\widehat{\mathbb{R}}} \xi |\widehat{g}(\xi)|^2 d\xi.$$

Proof. We make use of the fact that the expected value of a random variable X minimizes its variance, meaning

$$\mathbb{E} \{ |X - \mathbb{E}\{X\}|^2 \} \leq \mathbb{E} \{ |X - z|^2 \} \quad \text{for all } z \in \mathbb{C}.$$

Choosing $X = \widehat{h}(\Xi)$ as in Lemma 2.1 and $z = \widehat{h}(\mu_{|\widehat{g}|^2})$ we get

$$\begin{aligned} d_{g,h}^2 &= \mathbb{E} \{ |\widehat{h}(\Xi) - \mathbb{E}\{\widehat{h}(\Xi)\}|^2 \} \\ &\leq \mathbb{E} \{ |\widehat{h}(\Xi) - \widehat{h}(\mu)|^2 \} \\ &= \int_{\widehat{\mathbb{R}}} |\widehat{h}(\xi) - \widehat{h}(\mu)|^2 |\widehat{g}(\xi)|^2 d\xi \\ &\leq \int_{\widehat{\mathbb{R}}} (\|\widehat{h}'\|_{\mathbf{L}^\infty} |\xi - \mu|)^2 |\widehat{g}(\xi)|^2 d\xi \\ &= \|\widehat{h}'\|_{\mathbf{L}^\infty}^2 \sigma_{|\widehat{g}|^2}^2. \end{aligned}$$

By Bernstein's inequality (e.g., see [14], Ch. XVII, Thm. 7.24), $\text{supp } h \subseteq [-\frac{x_0}{2}, +\frac{x_0}{2}]$ implies

$$\|\widehat{h}'\|_{\mathbf{L}^\infty} \leq \pi x_0 \|\widehat{h}\|_{\mathbf{L}^\infty}.$$

Together with $\|\widehat{h}\|_{\mathbf{L}^\infty} = 1$ this proves the claim. \square

Remark. The upper bound in Proposition 2.2 does not make sense whenever the decay of $|\widehat{g}|$ is too slow (e.g., if g is not continuous). In that case, we can obtain a more conservative (though less elegant) bound from the following estimate.

Given an appropriate $\varepsilon > 0$, there is $\Omega > 0$ such that

$$\int_{|\xi| \leq \Omega} |\widehat{g}(\xi)|^2 d\xi = 1 - \varepsilon.$$

Then we can define

$$\widehat{g}_\Omega = \frac{1}{\sqrt{1-\varepsilon}} \chi_{[-\Omega, +\Omega]} \widehat{g}$$

which ensures that $|\widehat{g}_\Omega|^2$ is a probability density with finite variance. Along the same lines as in the proof of Proposition 2.2 (using $\mu = \mu_{|\widehat{g}_\Omega|^2}$), we obtain

$$d_g^2 \leq (\pi x_0)^2 \sigma_{|\widehat{g}_\Omega|^2}^2 (1 - \varepsilon) + 4\varepsilon.$$

Lower bound. On the other hand, one must expect that signals which are not well localized on the frequency side potentially undergo a relatively strong orthogonal perturbation. Clearly, for a given convolution operator there might be arbitrarily bad localized functions g which are exact eigenfunctions of this specific operator, so $d_{g,h} = 0$ for this particular h — but for practical purposes, we require a family of basis functions that are stable under the action of all $h \in \mathcal{H}$. Therefore, to be able to show that certain families are inadequate, we want to determine a lower bound for d_g . To this end, we shall use the following kind of uncertainty principle obtained by Slepian, Pollak, and Landau [9, 10, 11].

Lemma 2.3. *Let $f \in \mathbf{L}^2(\mathbb{R})$ with $\text{supp } f \subset [-\frac{T}{2}, +\frac{T}{2}]$. Then we have for all $\Omega > 0$ that*

$$\int_{-\Omega/2}^{+\Omega/2} |\widehat{f}(\xi)|^2 d\xi \leq \lambda_0 \|f\|^2,$$

where $\lambda_0 = \lambda_0(\Omega, T)$ is the square of the largest eigenvalue of the operator

$$\begin{aligned} O_{\Omega, T} : \mathbf{L}^2(\mathbb{R}) &\longrightarrow \mathbf{L}^2(\mathbb{R}), \\ f &\longmapsto \int_{-T/2}^{T/2} f(x) \frac{\sin(\pi\Omega(\cdot - x))}{\pi(\cdot - x)} dx. \end{aligned}$$

A scaling argument shows that λ_0 only depends on the product ΩT . The eigenfunctions of $O_{\Omega, T}$ are the so-called prolate spheroidal wave functions, which have been studied extensively as solutions of the second-order differential equation eigenvalue problem

$$\frac{d}{dx} \left((1-x^2) \frac{d\psi}{dx} \right) + (\lambda - c^2 x^2) \psi = 0$$

(e.g., see [7]).

We can obtain a somewhat weak upper bound on the operator norm of $O_{\Omega, T}$ using the following lemma [6], whose proof is included for the sake of completeness.

Lemma 2.4. (i) *Let $A \subset \mathbb{R}$ and $B \subset \widehat{\mathbb{R}}$ be sets of finite measure. Define the operator $P_A : \mathbf{L}^2(\mathbb{R}) \rightarrow \mathbf{L}^2(\mathbb{R})$, $f \mapsto \chi_A f$, and the operator $Q_B : \mathbf{L}^2(\mathbb{R}) \rightarrow \mathbf{L}^2(\mathbb{R})$, $f \mapsto (\chi_B \widehat{f})^\vee = \chi_B^\vee * f$. Then $\|Q_B P_A\|_{\mathcal{L}(\mathbf{L}^2)} \leq \sqrt{m(A) m(B)}$, where m denotes Lebesgue measure on \mathbb{R} .*

(ii) *For $f \in \mathbf{L}^2(\mathbb{R})$ with $\text{supp } f \subseteq [\alpha, \alpha + T]$ for some $\alpha \in \mathbb{R}$, we have*

$$\int_{-\Omega/2}^{+\Omega/2} |\widehat{f}(\xi)|^2 d\xi \leq \Omega T \|f\|_{\mathbf{L}^2}^2.$$

Proof. (i) Let $f \in \mathbf{L}^2(\mathbb{R})$. Using the Cauchy–Schwarz inequality and Fubini’s theorem, we obtain

$$\begin{aligned} \|Q_B P_A(f)\|^2 &= \int_{\mathbb{R}} \left| \int_{\mathbb{R}} \chi_A(y) f(y) \chi_B^\vee(x-y) dy \right|^2 dx \\ &\leq \int_{\mathbb{R}} (\|\chi_A\|_{\mathbf{L}^2} \|f(\cdot) \chi_B^\vee(x-\cdot)\|)^2 dx \\ &= m(A) \int_{\mathbb{R}} |f(y)|^2 \int_{\mathbb{R}} |\chi_B^\vee(x-y)|^2 dx dy \\ &= m(A) m(B) \|f\|_{\mathbf{L}^2}^2. \end{aligned}$$

(ii) Since $P_{[\alpha, \alpha+T]} f = f$, we have

$$\int_{-\Omega/2}^{+\Omega/2} |\widehat{f}(\xi)|^2 d\xi = \|(Q_{[-\frac{\Omega}{2}, +\frac{\Omega}{2}]}(f))^\wedge\|_{\mathbf{L}^2}^2 = \|Q_{[-\frac{\Omega}{2}, +\frac{\Omega}{2}]} P_{[\alpha, \alpha+T]} f\|_{\mathbf{L}^2}^2 \leq \Omega T \|f\|_{\mathbf{L}^2}^2.$$

□

In order to find a lower bound on d_g^2 , we construct a particular family of convolution operators K_h with $h \in \mathcal{H}$.

Lemma 2.5. *There exist constants $s \in]0, 1[$ and $r \in [\frac{1}{2}, 1[$ such that for any $N \in \mathbb{N}$, there is $h_N \in \mathcal{H}$ with*

$$(2.3) \quad \widehat{h}_N \leq \widehat{k} \quad \text{on } [-\frac{2N-1}{x_0}, 0] \quad \text{and} \quad \widehat{h}_N \geq \widehat{k} \quad \text{on } [0, +\frac{2N-1}{x_0}],$$

where $\widehat{k} : \mathbb{R} \rightarrow \mathbb{R}$ is given by

$$\widehat{k}(\xi) = \begin{cases} -r, & \text{for } \xi \leq -\frac{s}{x_0}, \\ r \frac{x_0}{s} \xi, & \text{for } \xi \in [-\frac{s}{x_0}, +\frac{s}{x_0}], \\ +r, & \text{for } \xi \geq +\frac{s}{x_0} \end{cases}$$

(compare Figure 2).

Proof. Without loss of generality, we may assume that $x_0 = 1$; the general case follows easily by dilation.

Consider the Bartlett window (“triangle function”)

$$\varphi(x) = (2 - 4|x|) \cdot \chi_{[-\frac{1}{2}, +\frac{1}{2}]}(x)$$

with Fourier transform

$$\widehat{\varphi}(\xi) = \left(\frac{\sin(\pi\xi/2)}{\pi\xi/2} \right)^2 = \text{sinc}^2\left(\frac{\pi\xi}{2}\right).$$

Obviously, $\varphi \in \mathcal{H}$. Note that $\widehat{\varphi}$ has the interpolation property

$$\widehat{\varphi}(2n) = \delta_{0,n} \quad \text{for } n \in \mathbb{Z}.$$

We use $\widehat{\varphi}$ to interpolate the sequence

$$(\dots, 0, 0, 0, \underbrace{-1, -1, \dots, -1, -1}_N, \underbrace{+1, +1, \dots, +1, +1}_N, 0, 0, 0, \dots)$$

on the odd integers, obtain

$$\widehat{h}_N = \sum_{n=1}^N \widehat{\varphi}(\xi - (2n-1)) - \widehat{\varphi}(\xi + (2n-1)),$$

and claim that this \widehat{h}_N satisfies the inequalities (2.3).

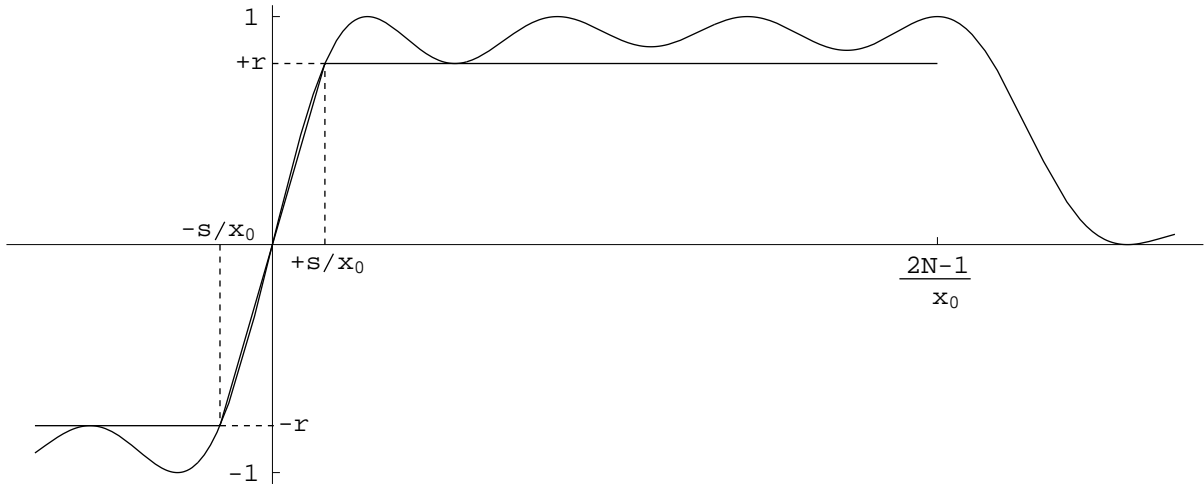


FIGURE 2. Graphs of \widehat{h}_N and \widehat{k} .

For $\xi \in [1, 2N-1]$, we have $\frac{\xi-1}{2} + n \geq n$, so

$$\sum_{n=1}^N \widehat{\varphi}(\xi + (2n-1)) = \sum_{n=1}^N \text{sinc}^2\left(\pi\left(\frac{\xi-1}{2} + n\right)\right) \leq \sum_{n=1}^N \frac{1}{\pi^2 n^2} \leq \frac{1}{6}.$$

On the other hand, making use of the identity

$$\sum_{n \in \mathbb{Z}} \operatorname{sinc}^2(\pi(t-n)) \equiv 1,$$

we have for $\xi \in [1, 2N-1]$, i.e., $\frac{\xi+1}{2} \in [1, N]$,

$$\begin{aligned} \sum_{n=1}^N \widehat{\varphi}(\xi - (2n-1)) &= \sum_{n=1}^N \operatorname{sinc}^2\left(\pi\left(\frac{\xi+1}{2}-n\right)\right) \\ &= 1 - \sum_{n=-\infty}^0 \operatorname{sinc}^2\left(\pi\left(\frac{\xi+1}{2}-n\right)\right) - \sum_{n=N+1}^{\infty} \operatorname{sinc}^2\left(\pi\left(\frac{\xi+1}{2}-n\right)\right) \\ &\geq 1 - \sum_{n=-\infty}^0 \frac{1}{\pi^2(1-n)^2} - \sum_{n=N+1}^{\infty} \frac{1}{\pi^2(N-n)^2} = 1 - \frac{1}{6} - \frac{1}{6} = \frac{2}{3}. \end{aligned}$$

Consequently,

$$\widehat{h}_N(\xi) = \sum_{n=1}^N \operatorname{sinc}^2\left(\pi\left(\frac{\xi+1}{2}-n\right)\right) - \sum_{n=1}^N \operatorname{sinc}^2\left(\pi\left(\frac{\xi-1}{2}+n\right)\right) \geq \frac{2}{3} - \frac{1}{6} = \frac{1}{2} \quad \text{for } \xi \in [1, 2N-1].$$

For $\xi \in [0, 1]$, we use $\sin^2\left(\frac{\pi}{2}(\xi-2n+1)\right) = \sin^2\left(\frac{\pi}{2}(\xi+2n-1)\right) = \cos^2\left(\frac{\pi}{2}\xi\right)$ to obtain

$$\begin{aligned} \widehat{h}_N(\xi) &= \sum_{n=1}^N \frac{\sin^2\left(\pi\left(\frac{\xi+1}{2}-n\right)\right)}{\pi^2\left(\frac{\xi+1}{2}-n\right)^2} - \frac{\sin^2\left(\pi\left(\frac{\xi-1}{2}+n\right)\right)}{\pi^2\left(\frac{\xi-1}{2}+n\right)^2} \\ &= \frac{\cos^2\left(\frac{\pi}{2}\xi\right)}{\pi^2} \sum_{n=1}^N \left(\frac{1}{\left(\frac{\xi-2n+1}{2}\right)^2} - \frac{1}{\left(\frac{\xi+2n-1}{2}\right)^2} \right)^2 \\ &= \frac{\cos^2\left(\frac{\pi}{2}\xi\right)}{\pi^2} \sum_{n=1}^N 4 \frac{(\xi+2n-1)^2 - (\xi-2n+1)^2}{(\xi-2n+1)^2(\xi+2n-1)^2} \\ &= \sum_{n=1}^N \frac{16 \cos^2\left(\frac{\pi}{2}\xi\right) \xi (2n-1)}{\pi^2((2n-1)^2 - \xi^2)^2}. \end{aligned}$$

Since for $\xi \geq 0$, each summand is nonnegative, we see that

$$\widehat{h}_N(\xi) \geq \widehat{h}_1(\xi) = \left(\frac{4 \cos\left(\frac{\pi}{2}\xi\right)}{\pi(1-\xi^2)} \right)^2 \xi \quad \text{for } \xi \in [0, 1].$$

Furthermore, $\sin\left(\frac{\pi}{2}\xi\right) \geq \xi$ on $[0, 1]$ implies

$$\cos\left(\frac{\pi}{2}\xi\right) = \int_{\xi}^1 \frac{\pi}{2} \sin\left(\frac{\pi}{2}\eta\right) d\eta \geq \int_{\xi}^1 \frac{\pi}{2} \eta d\eta = \frac{\pi}{4} (1 - \xi^2) \geq 0 \quad \text{for } \xi \in [0, 1],$$

so we know that $\frac{4 \cos\left(\frac{\pi}{2}\xi\right)}{\pi(1-\xi^2)} \geq 1$, i.e.,

$$\widehat{h}_N(\xi) \geq \xi \quad \text{for } \xi \in [0, 1].$$

Since the sinc^2 -function is even, the functions \widehat{h}_N are odd, so \widehat{h}_N satisfies the conditions stated in the lemma for $r = s = \frac{1}{2}$.

It remains to show that $h_N \in \mathcal{H}$. Since $\widehat{h}_N = \sum_n a_n \tau_n \widehat{\varphi}$ is equivalent to $h_N = \sum_n a_n e^{2\pi i n x} \varphi$, we have $\operatorname{supp} h_N \subseteq \operatorname{supp} \varphi = [-\frac{1}{2}, +\frac{1}{2}]$. By construction, \widehat{h}_N is real valued

and odd, so h_N is (imaginary valued and) odd, which implies that $|h_N|^2$ is even and therefore has vanishing first moment. Finally, since $\widehat{\varphi} \geq 0$, we have

$$|\widehat{h}_N(\xi)| \leq \sum_{n=1}^N \widehat{\varphi}(\xi - (2n+1)) + \widehat{\varphi}(\xi + (2n-1)) \leq \sum_{n \in \mathbb{Z}} \text{sinc}^2\left(\pi\left(\frac{\xi+1}{2} - n\right)\right) = 1$$

with $\widehat{h}_N(1) = 1$ by the interpolating properties of $\widehat{\varphi}$, so $\|\widehat{h}_N\|_{\mathbf{L}^\infty} = 1$. \square

Remark. It is worth noting that the above estimates are rather crude. Numerical experiments show that we actually have $r \doteq 0.8$ and $s \doteq 0.56$ for $N \geq 7$. An alternative approach is interpolation with the sinc-function itself of the sequence

$$(\dots, 0, 0, -\frac{1}{2}, -1, -1, \dots, -1, 0, +1, \dots, +1, +1, +\frac{1}{2}, 0, 0, \dots)$$

on the integers. This yields $r \doteq 0.900$ and $s \doteq 0.956$.

Proposition 2.6. *For $g \in \mathbf{L}^2(\mathbb{R})$, $\|g\|_{\mathbf{L}^2} = 1$, with $\text{supp } g \subseteq [\alpha, \alpha + T]$ for some $\alpha \in \mathbb{R}$ and $T > 0$, we have*

$$\begin{aligned} d_g^2 &\geq r^2 \left(1 - \frac{4}{3} s \frac{T}{x_0}\right) && \text{for } \frac{T}{x_0} \leq \frac{1}{2s}, \\ \text{and } d_g^2 &\geq \frac{1}{12} \left(\frac{r x_0}{s T}\right)^2 && \text{for } \frac{T}{x_0} > \frac{1}{2s}, \end{aligned}$$

where r and s are the constants from Lemma 2.5.

Proof. Let $g \in \mathbf{L}^2(\mathbb{R})$ have the assumed properties and recall that

$$d_{g,h}^2 = \mathbb{E} \left\{ \left| \widehat{h}(\Xi) - \mathbb{E}\{\widehat{h}(\Xi)\} \right|^2 \right\},$$

where Ξ is a random variable with probability density $|\widehat{g}|^2$. The family \mathcal{H} is invariant under modulation, i.e., we may translate \widehat{h} by any $\xi \in \widehat{\mathbb{R}}$ without leaving \mathcal{H} . We know by Lemma 2.5 that $\widehat{h}_N \geq \frac{1}{2}$ on $[\frac{1}{x_0}, \frac{2N-1}{x_0}]$, so after fixing $M > 0$ such that

$$\int_{|\xi| \leq M} |\widehat{g}(\xi)|^2 d\xi > \frac{2}{3},$$

we have for $N \geq Mx_0 + 1$

$$\begin{aligned} \mathbb{E} \left\{ \left(\tau_{-(M+\frac{1}{x_0})} \widehat{h}_N \right) (\Xi) \right\} &= \int_{\widehat{\mathbb{R}}} \widehat{h}_N(\xi + M + \frac{1}{x_0}) |\widehat{g}(\xi)|^2 d\xi \\ &\geq \int_{|\xi| \leq M} \widehat{h}_N(\xi + M + \frac{1}{x_0}) |\widehat{g}(\xi)|^2 d\xi - \left| \int_{|\xi| > M} \widehat{h}_N(\xi + M + \frac{1}{x_0}) |\widehat{g}(\xi)|^2 d\xi \right| \\ &> \frac{1}{2} \cdot \frac{2}{3} - 1 \cdot \frac{1}{3} = 0, \end{aligned}$$

and analogously, by symmetry,

$$\mathbb{E} \left\{ \left(\tau_{+(M+\frac{1}{x_0})} \widehat{h}_N \right) (\Xi) \right\} < 0.$$

Since \widehat{h}_N is a real-valued element of $\mathbf{L}^1(\mathbb{R}, |\widehat{g}|^2)$ and the group of translations acts continuously on this space, there exists $\xi_N \in]-(M+\frac{1}{x_0}), +(M+\frac{1}{x_0})[$ such that

$$\mathbb{E} \left\{ \left(\tau_{\xi_N} \widehat{h}_N \right) (\Xi) \right\} = 0.$$

Letting $\widehat{h}_N^* = \tau_{\xi_N} \widehat{h}_N$, we obtain (for N sufficiently large)

$$\begin{aligned} d_g^2 &\geq d_{g, \widehat{h}_N^*}^2 = \mathbb{E} \left\{ \left| \widehat{h}_N^*(\Xi) - \mathbb{E}\{\widehat{h}_N^*(\Xi)\} \right|^2 \right\} \\ &= \mathbb{E} \left\{ \left| \widehat{h}_N^*(\Xi) \right|^2 \right\} = \int_{\widehat{\mathbb{R}}} |\widehat{h}_N^*(\xi)|^2 |\widehat{g}(\xi)|^2 d\xi \end{aligned}$$

$$\begin{aligned}
&= \int_{\widehat{\mathbb{R}}} |\widehat{h}_N(\xi)|^2 |\widehat{g}(\xi + \xi_N)|^2 d\xi \geq \int_{|\xi| \leq \frac{2N-1}{x_0}} |\widehat{k}(\xi)|^2 |\widehat{g}(\xi + \xi_N)|^2 d\xi \\
&\geq \left(\int_{|\xi| \leq \frac{s}{x_0}} (r \frac{x_0}{s} \xi)^2 |\widehat{g}(\xi + \xi_N)|^2 d\xi + \int_{\frac{s}{x_0} \leq |\xi| \leq \frac{2N-1}{x_0}} r^2 |\widehat{g}(\xi + \xi_N)|^2 d\xi \right) \\
&= r^2 \left(\int_{|\xi| \leq \frac{s}{x_0}} \left(\int_0^{(\frac{x_0}{s} \xi)^2} 1 dt \right) |\widehat{g}(\xi + \xi_N)|^2 d\xi + \int_{\frac{s}{x_0} \leq |\xi| \leq \frac{2N-1}{x_0}} |\widehat{g}(\xi + \xi_N)|^2 d\xi \right) \\
&= r^2 \left(\int_0^1 \int_{\frac{s}{x_0} \sqrt{t} \leq |\xi| \leq \frac{s}{x_0}} |\widehat{g}(\xi + \xi_N)|^2 d\xi dt + \int_{\frac{s}{x_0} \leq |\xi| \leq \frac{2N-1}{x_0}} |\widehat{g}(\xi + \xi_N)|^2 d\xi \right) \\
&= r^2 \int_0^1 \int_{\frac{s}{x_0} \sqrt{t} \leq |\xi| \leq \frac{2N-1}{x_0}} |\widehat{g}(\xi + \xi_N)|^2 d\xi dt \\
&= r^2 \int_0^1 \left(1 - \int_{|\xi| \leq \frac{s}{x_0} \sqrt{t}} |\widehat{g}(\xi + \xi_N)|^2 d\xi - \int_{|\xi| \geq \frac{2N-1}{x_0}} |\widehat{g}(\xi + \xi_N)|^2 d\xi \right) dt \\
&\geq r^2 \int_0^a \left(1 - \int_{|\xi| \leq \frac{s}{x_0} \sqrt{t}} |\widehat{g}(\xi + \xi_N)|^2 d\xi - \int_{|\xi| \geq \frac{2N-1}{x_0}} |\widehat{g}(\xi + \xi_N)|^2 d\xi \right) dt
\end{aligned}$$

for $a \leq 1$. Since translation of \widehat{g} does not change the support of g , we may apply Lemma 2.4.(ii) and obtain

$$\int_{|\xi| \leq \frac{s}{x_0} \sqrt{t}} |\widehat{g}(\xi + \xi_N)|^2 d\xi \leq (2 \frac{s}{x_0} \sqrt{t}) \cdot T.$$

Furthermore, since $|\xi_N| \leq M + \frac{1}{x_0}$, we have

$$\int_{|\xi| \geq \frac{2N-1}{x_0}} |\widehat{g}(\xi + \xi_N)|^2 d\xi \rightarrow 0 \quad \text{as } N \rightarrow \infty.$$

For $\frac{T}{x_0} \leq \frac{1}{2s}$ we choose $a = 1$ and obtain

$$d_g^2 \geq r^2 \int_0^1 \left(1 - 2 \frac{s}{x_0} \sqrt{t} T \right) dt = r^2 \left(1 - \frac{4}{3} \frac{sT}{x_0} \right);$$

for $\frac{T}{x_0} > \frac{1}{2s}$, letting $a = (\frac{x_0}{2sT})^2$ yields

$$d_g^2 \geq \frac{1}{12} \left(\frac{r x_0}{s T} \right)^2.$$

□

Remark. To obtain a lower bound for d_g^2 in Proposition 2.6, we used the upper bound for $\|Q_B P_A\|_{\mathcal{L}(\mathbf{L}^2)}$ from Lemma 2.4. But for the case $B = [-\frac{\Omega}{2}, +\frac{\Omega}{2}]$ and $A = [T, T + \alpha]$, Lemma 2.3 provides a sharp upper bound of $\|Q_B P_A\|_{\mathcal{L}(\mathbf{L}^2)} = \|O_{\Omega, T}\|_{\mathcal{L}(\mathbf{L}^2)}$ in terms of the largest eigenvalue $\sqrt{\lambda_0(\Omega, T)}$ of the operator $O_{\Omega, T}$. Since this eigenvalue only depends on the product of Ω and T , we shall write $\lambda_0(\Omega, T) = \lambda_0(\Omega \cdot T)$. If in the proof of Proposition 2.6, we use this sharp bound, we get

$$d_g^2 \geq r^2 \int_0^1 1 - \lambda_0((2 \frac{s}{x_0} \sqrt{t}) \cdot T) dt.$$

The graph of this lower bound for d_g^2 (dashed) as well as the graph of that obtained in Proposition 2.6 (solid line) are shown in Figure 3 for $s = 0.956$ and $r = 0.9$.

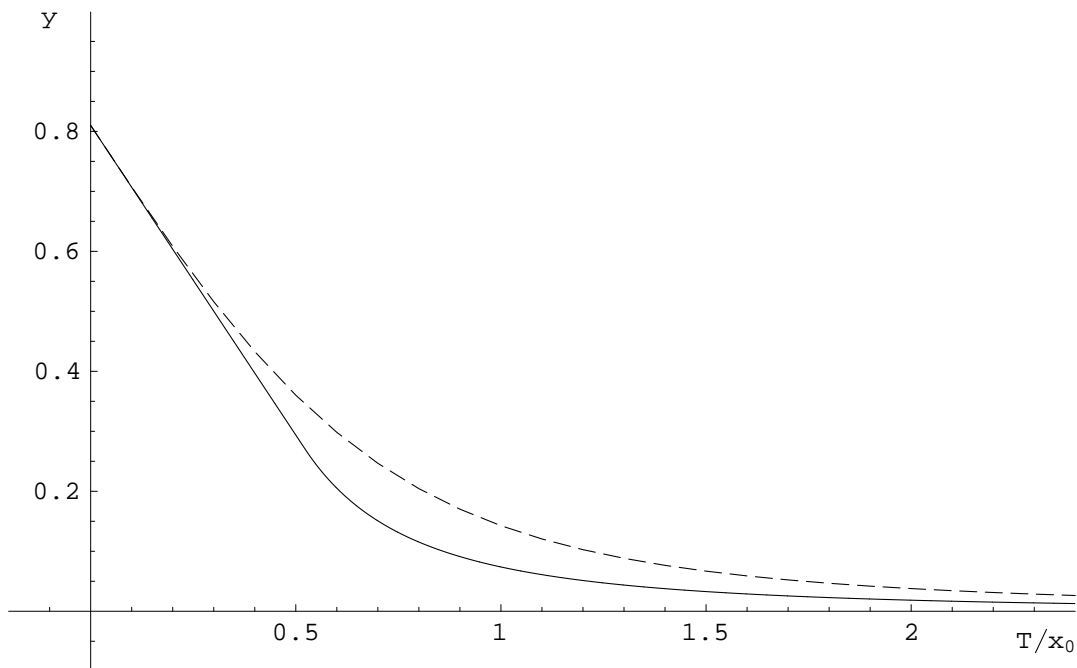


FIGURE 3. Lower bounds for d_g^2 .

We also should note that $\sqrt{\lambda_0(\Omega \cdot T)}$ is always a simple eigenvalue of the operator $O_{\Omega, T}$. For $\Omega \cdot T < 1$ (i.e., $\frac{T}{x_0} < \frac{1}{2s}$), the second largest eigenvalue is already considerably smaller. This reflects the fact that only a number of about $\Omega \cdot T$ linearly independent functions have “approximate duration” $[0, T]$ and “approximate bandwidth” $[-\frac{\Omega}{2}, +\frac{\Omega}{2}]$ (see [11]). Consequently, we see that unless we use for g the appropriate spheroidal wave function itself, d_g^2 will be significantly bigger than the bound given above.

3. ORTHOGONAL PERTURBATIONS OF COHERENT FAMILIES

We now want to compare the three types of coherent families described at the beginning with respect to their performance under orthogonal perturbation. As for the parameters, we assume $\text{supp } h \subseteq [-\frac{x_0}{2}, +\frac{x_0}{2}]$ and

$$a = 50 x_0 .$$

Furthermore, we will use

$$r \doteq 0.9 \quad \text{and} \quad s \doteq 1$$

for the function \widehat{k} from Lemma 2.5 (compare the remark after its proof).

As for the number of elements N in the family, $N \geq 256$ seems realistic; in VDSL applications, $N \approx 2000$ is used.

3.1. Weyl–Heisenberg families. Recall that a Weyl–Heisenberg family is generated by fixing a basic function g_0 with $\text{supp } g_0 \subseteq [0, a]$ and then letting $g_l(x) = g_0(x) e^{2\pi i b l x}$. Thus we have $\text{supp } g_l = \text{supp } g_0$ and $|\widehat{g}_l|^2 = \tau_{bl} |\widehat{g}_0|^2$. Since the variance is translation invariant, we have $\sigma_{|\widehat{g}_l|^2}^2 = \sigma_{|\widehat{g}_0|^2}^2$ for all g_l , so the upper bound from Proposition 2.2 holds uniformly in $h \in \mathcal{H}$ and $l = 0 \dots N-1$.

Using for g_0 a triangle function, a trapezoidal function, or the polynomial $x^2(x - a)^2$ (properly normalized) yields

$$d_g^2 \doteq 0.0012 .$$

It is worth emphasizing that the main property ensuring this uniform upper bound is the fact that within a Weyl–Heisenberg family, all \widehat{g}_t share the same frequency localization.

3.2. Wilson bases. In a Wilson basis, we start from a basic function g with $\text{supp } g \subseteq [0, a]$. The Fourier transforms of the elements satisfy

$$(3.1) \quad |\widehat{g}_m^{(j)}(\xi)|^2 = \frac{1}{2} |\widehat{g}(\xi + \xi_0) \pm \widehat{g}(\xi - \xi_0)|^2,$$

in particular, for $j = 1$ we have “+” and $\xi_0 = \frac{2m}{a}$. Thus the variance of $|\widehat{g}_m^{(1)}|^2$ increases with m . Using the appropriate $h_N \in \mathcal{H}$ from Lemma 2.5 shows that the orthogonal perturbation turns bad quickly, as the following result shows (compare Figure 4).

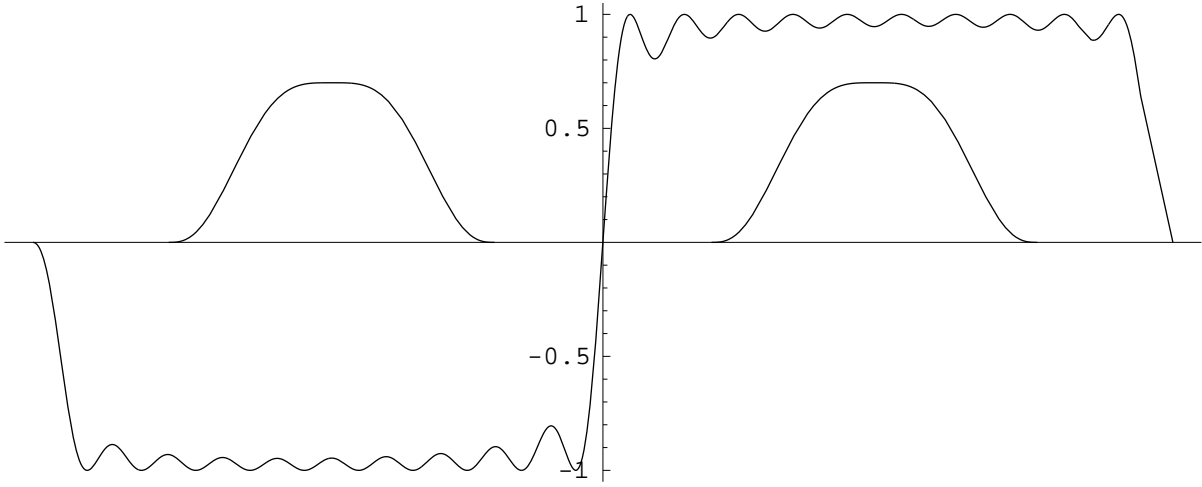


FIGURE 4. Graphs of \widehat{h}_N and $|\widehat{g}_m^{(j)}|^2$ for large m in a Wilson basis.

Theorem 3.1. *In a Wilson basis with at least 200 elements and $\text{supp } g_0 \subseteq [0, a]$, there is an element g_t with*

$$d_{g_t}^2 \geq \frac{r^2}{5} \doteq 0.16.$$

Proof. Consider first the function g_0 with $\|g_0\|_{\mathcal{L}^2(\mathbb{R})} = 1$. If $d_{g_0}^2 \geq \frac{r^2}{5}$, there is nothing to prove. If not, we will make use of the functions h_N from Lemma 2.5; by construction, these are odd. Since the $g_m^{(j)}$ are real-valued, we know that $|\widehat{g}_m^{(j)}|^2$ is even, so $\text{E}\{\widehat{h}_N(\Xi)\} = 0$. Therefore, $d_{g_m^{(j)}, h_N}^2 = \text{V}\{\widehat{h}_N(\Xi)\} = \text{E}\{|\widehat{h}_N(\Xi)|^2\}$. For g_0 , this implies

$$\frac{r^2}{5} \geq d_{g_0}^2 \geq \int_{\mathbb{R}} |\widehat{k}(\xi)|^2 |\widehat{g}_0(\xi)|^2 d\xi \geq \int_{|\xi| \geq 1/x_0} r^2 |\widehat{g}_0(\xi)|^2 d\xi,$$

i.e., $\int_{|\xi| \geq 1/x_0} |\widehat{g}_0(\xi)|^2 d\xi \leq \frac{1}{5}$. Splitting \widehat{g}_0 into the center part $\widehat{g}_c = \widehat{g}_0 \cdot \chi_{[-1/x_0, +1/x_0]}$ and the tails $\widehat{g}_t = \widehat{g}_0 - \widehat{g}_c$, we have $\|\widehat{g}_c\|_{\mathcal{L}^2}^2 \geq \frac{4}{5}$ and $\|\widehat{g}_t\|_{\mathcal{L}^2}^2 \leq \frac{1}{5}$.

If the basis has at least 200 elements, we have to allow $m \geq 50$, so for $j = 1$, the value ξ_0 in (3.1) becomes $\xi_0 = \frac{2m}{a} \geq \frac{2}{x_0}$. Thus we can estimate

$$\begin{aligned} \int_{|\xi| \geq 1/x_0} |\widehat{g}_{m,1}(\xi)|^2 d\xi &\geq \int_{|\xi - \xi_0| \leq 1/x_0} \frac{1}{2} |\widehat{g}_0(\xi - \xi_0) + \widehat{g}_0(\xi + \xi_0)|^2 d\xi \\ &\geq \frac{1}{2} (\|g_c\| - \|g_t\|)^2 \geq \frac{1}{2} \left(\frac{2}{\sqrt{5}} - \frac{1}{\sqrt{5}} \right)^2 = \frac{1}{10}. \end{aligned}$$

By symmetry, the same estimate holds for the integral over the set $\{|\xi + \xi_0| \leq 1/x_0\}$, and we obtain for N sufficiently large (namely, for $\frac{2N-1}{x_0} \geq \xi_0 + \frac{1}{x_0}$)

$$d_{g_m^{(1)}, h_N}^2 = \mathbb{E}\{|\widehat{h}_N(\Xi)|^2\} \geq \frac{1}{10}(-r)^2 + \frac{1}{10}(+r)^2,$$

which yields the claim. \square

3.3. Wavelet bases. In a dyadic wavelet basis, we encounter the problem that, since scaling on the time side results in reverse scaling on the frequency side, the frequency localization gets worse and worse as the indices grow (compare figure 5). The following result gives a quantitative estimate of this effect.

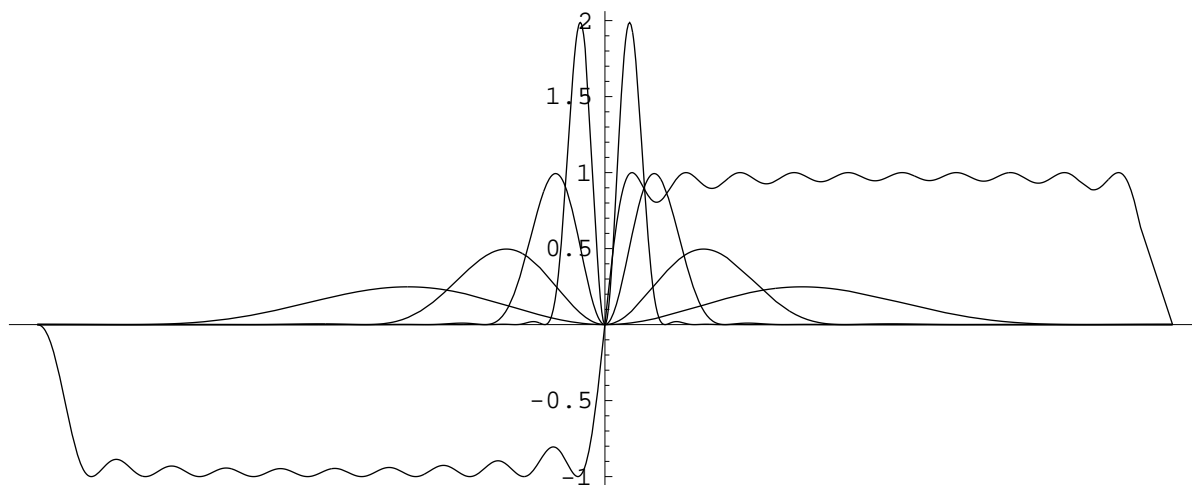


FIGURE 5. Graphs of \widehat{h}_N and $|\widehat{g}_m^{(n)}|^2$ for various m in a wavelet basis.

Theorem 3.2. *In a dyadic wavelet family with $\text{supp } g_0 \subseteq [0, Ka]$ and finest scaling level $M \geq 7 + \log_2(K)$, the elements $g_M^{(n)}$ on level M satisfy*

$$d_{g_M^{(n)}}^2 \geq 0.81 (1 - 67 \cdot 2^{-M} K).$$

Proof. The property $\text{supp } g_0 \subseteq [0, Ka]$ implies $\text{supp } g_M^{(n)} \subseteq [n 2^{-M} Ka, (n+1) 2^{-M} Ka]$. For $M \geq 7 + \log_2(K)$, we have $\frac{2^{-M} Ka}{x_0} \leq \frac{50}{128} < \frac{1}{2s}$, so Proposition 2.6 yields

$$d_{g_M^{(n)}}^2 \geq r^2 \left(1 - \frac{4}{3} s \frac{2^{-M} Ka}{x_0}\right) = 0.9^2 \left(1 - \frac{200}{3} 2^{-M} K\right).$$

\square

When using the orthogonal Daubechies wavelet with four vanishing moments (db4 in MatLab), we may choose $K = 8$. If $N > 1024$, we need $M \geq 11$ which yields $d_{g_{11}^{(n)}}^2 \geq 0.386$; for $N > 2048$ with $M \geq 12$ we obtain $d_{g_{12}^{(n)}}^2 \geq 0.598$.

Remark. The numerical results presented above demonstrate very clearly that the Weyl–Heisenberg systems outperform the other two types of coherent families by far. Standardized implementations of so-called multicarrier communication systems such as OFDM (orthogonal frequency division multiplex) or DMT (discrete multi-tone) are based on the Weyl–Heisenberg structure using indicator functions of different lengths at the transmitter and receiver [8, 13]. There, the transmission basis is usually defined as

$$g_{k,l}(x) = \chi_{[-x_0, T]}(x - ak) e^{2\pi i b l x},$$

where $a = T+x_0$ and $b = 1/T$; i.e., a nonorthogonal Riesz basis whose span covers functions that contain a so-called *cyclic prefix* of length x_0 . This means that within the interval $[kT-x_0, kT+T]$, one has $f(x) = f(x+T)$ for $x \in [kT-x_0, kT]$. The dual basis at the receiver can be interpreted to be cutting off the *cyclic prefix*, since

$$\gamma_{k,l}(x) = \chi_{[0,T]}(x-ak) e^{2\pi i b l x}.$$

It is straightforward to prove exact diagonalization of convolution operators with h supported in $[0, x_0]$ by this biorthogonal system, i.e., we have

$$\langle K_h g_{k,l}, \gamma_{k',l'} \rangle = \widehat{h}\left(\frac{l}{T}\right) \delta_{k,k'} \delta_{l,l'}.$$

However, such an exact diagonalization has two disadvantages. On the one hand, it wastes bandwidth, since the space $\overline{\text{span}}\{g_{k,l}\}_{k \in \mathbb{Z}, l=1 \dots N}$ shrinks with increasing x_0 . This effect again becomes negligible when using a large number of tones (large N) and a correspondingly long signal duration a . On the other hand, the use of an indicator function implies bad frequency localization of the basis functions, this disadvantage can be reduced by employing pulse shaping [12]. A more detailed discussion of this and other tradeoffs in the design of Weyl–Heisenberg structured signal sets for digital communication can be found in [3] and the references therein.

4. CHANNEL MATRICES

To illustrate the results of Section 2 in a realistic setup, we shall compute the channel matrix of different exemplary transmission bases with respect to a normalized convolution operator reflecting a 2km, 0.4mm PE twisted copper wire cable.

Given an orthonormal basis $\{e_i\}_{i \in I}$ of the Hilbert space $L^2(\mathbb{R})$ and any bounded operator $K : L^2(\mathbb{R}) \rightarrow L^2(\mathbb{R})$, we define the bi-infinite Gram matrix G^K through

$$G_{i,j}^K = \langle K e_i, e_j \rangle, \quad i, j \in I.$$

The Gram matrix leads to a matrix representation of the operator K : For all $f = \sum_{i \in I} c_i e_i \in L^2(\mathbb{R})$ we have $Kf = \sum_{j \in I} \tilde{c}_j e_j$ with

$$\tilde{c}_j = \langle Kf, e_j \rangle = \sum_i c_i \langle K e_i, e_j \rangle = \sum_i c_i G_{i,j}^K, \quad j \in I,$$

that is, $\tilde{c} = c \cdot G^K$. As a direct consequence of the definition of G^K and the orthonormality of the family $\{e_i\}$, we have

$$d_{e_i, K}^2 = \sum_{j \neq i} |G_{i,j}^K|^2.$$

In the transmission systems discussed here, we use an orthonormal family $\{g_i\}_{i \in I'}$ which is not complete in $L^2(\mathbb{R})$. Furthermore, the operator is a convolution operator K_h which is characterized by its impulse response. Adjusting the definition of the Gram matrix, we define the channel matrix $G_{i,j}^h = \langle K_h g_i, g_j \rangle$, $i, j \in I'$, and get

$$d_{g_i, K}^2 \geq \sum_{j \neq i} |G_{i,j}^K|^2.$$

In order to visualize the channel matrices, we choose a logarithmic scale, i.e., we plot $\log |G_{i,j}^h|$ and use the gray scale which is shown in Figure 8.

To compare the families discussed within a setting similar to ADSL, we choose $a \approx 1000 \mu\text{s}$ and bases capable of transmitting about 2000 real coefficients (1000 imaginary coefficients) utilizing the baseband $[-1, 1]$ MHz.

The impulse response of a 2km, 0.4mm PE twisted copper wire cable sampled at 2 MHz has been calculated according to [1]. The resulting causal impulse response

has been shifted to improve the performance of all the coherent families discussed here. Additionally, the impulse response has been normalized so that $\sup |\widehat{h}(\gamma)| = 1$. The resulting function h is shown in Figure 6. Figure 7 shows the real and the imaginary part

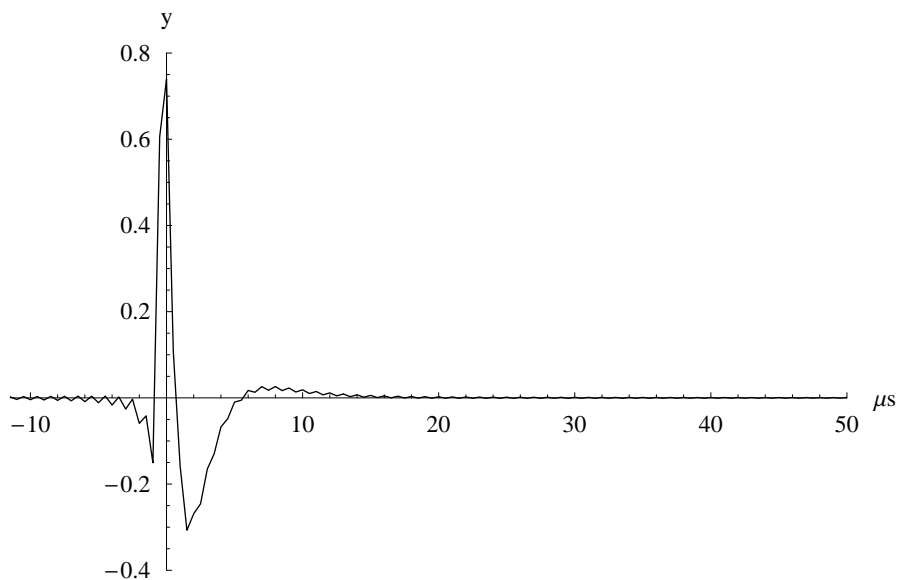


FIGURE 6. Channel impulse response h of a 2km 0,4mm PE twisted copper wire cable.

of the transfer function of K_h , i.e., $\text{Re}(\widehat{h})$ and $\text{Im}(\widehat{h})$.

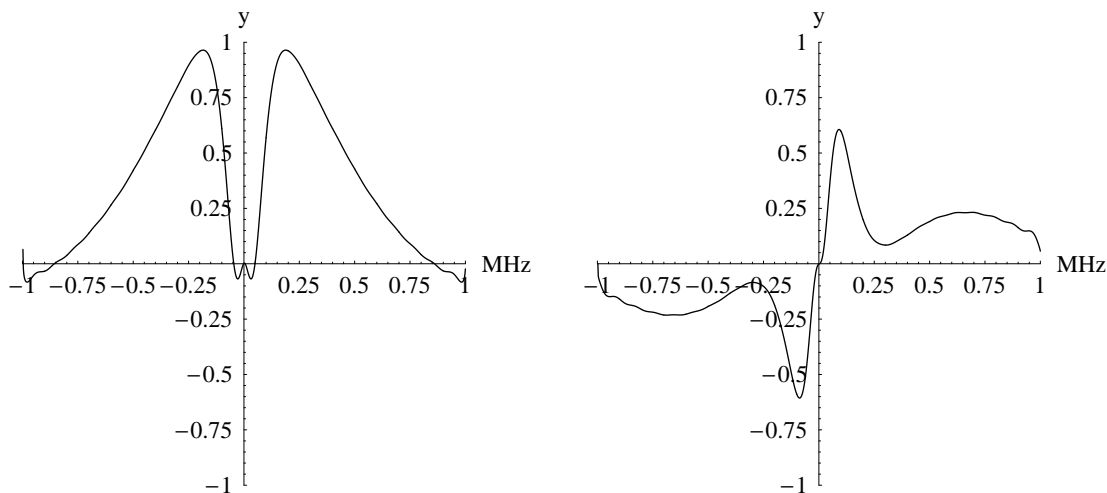


FIGURE 7. Real and Imaginary part of the transfer function \widehat{h} .

4.1. **Weyl–Heisenberg families.** We take the normalized characteristic function

$$g_0(t) = \frac{1}{\sqrt{1000}} \chi_{[0,1000)}(t [\mu\text{s}])$$

as prototype function and we choose the constants $a = 1000\mu\text{s}$, $b = \frac{1}{1000}\text{MHz}$ and $L = 1000$.

To illustrate the perturbation characteristics of this system we reorder and renumber the basis elements according to

$$g_{l+1000k} = g_{l,k}, \quad l = 0, \dots, 999, \quad k \in \mathbb{Z}$$

and calculate the channel matrix $G_{i,j}^h = \langle K_h g_i, g_j \rangle$, for $0 < i < 999$ and $-1000 < j < 1999$. In Figure 9 we display $\log |G_{i,j}^h|$ for $0 < i < 999$, $1000 < j < 1999$. The restriction to this segment of the biinfinite channel matrix is justified, since, due to the translation invariance of the convolution operator K_h , we have $G_{i,j}^h = G_{i+1000,j+1000}^h$ and, assuming $\text{supp } h \in [-1000, 1000]\mu\text{s}$ we have $G_{i,j}^h = 0$ for $|i - j| > 1000$. The dominance of the

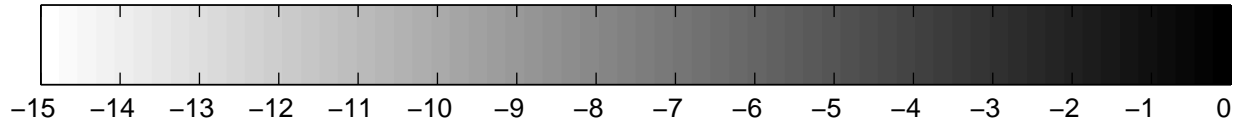


FIGURE 8. Gray scale used in the channel matrix images of Figures 9–18.

diagonal of this matrix demonstrates the channel perturbation stability of this basis. Two segments of Figure 9 are displayed in Figure 10.

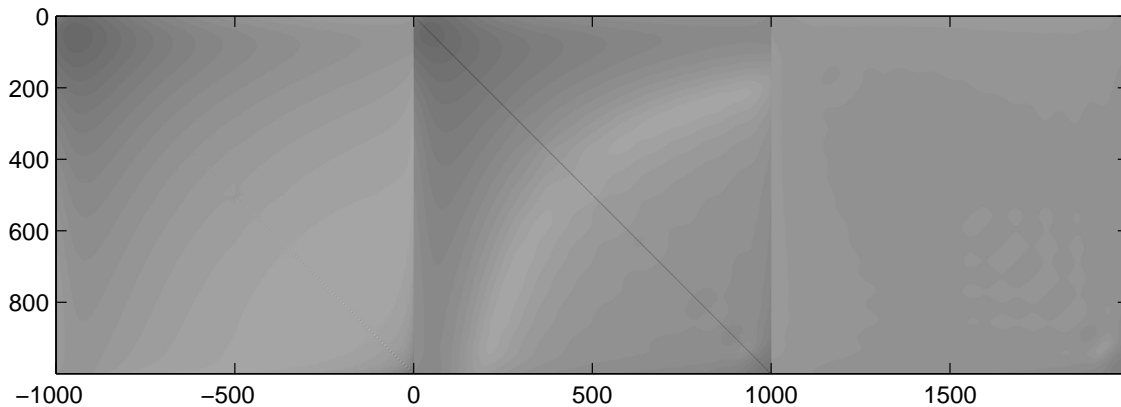


FIGURE 9. Channel matrix of a Weyl–Heisenberg family.

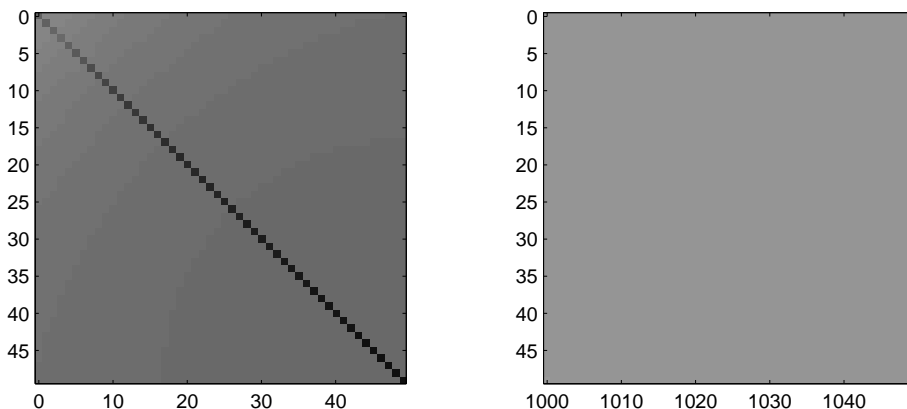


FIGURE 10. Details of Figure 9

To demonstrate the effect of the *cyclic prefix* described in the Remark in Section 3, we add a *cyclic prefix* of $30\mu\text{s}$ in the setting described above, i.e., we set

$$g_0(t) = \frac{1}{\sqrt{1000}} \chi_{[-30,1000]}(t [\mu\text{s}])$$

and choose

$$\gamma_0(t) = \frac{1}{\sqrt{1000}} \chi_{[0,1000)}(t [\mu\text{s}]).$$

In this case, the channel matrix is defined by

$$G_{i,j}^K = \langle K e_i, \gamma_j \rangle.$$

Due to the fact that $\{\gamma_j\}_{j \neq i}$ is an orthonormal family orthogonal to e_i ,

$$d_{e_i,h}^2 \geq \sum_{j,j \neq i} |G_{i,j}^h|^2$$

still holds. Using again $a = 1000\mu\text{s}$, $b = \frac{1}{1000}\text{MHz}$ and $L = 1000$, we obtain the channel matrix displayed in Figure 11. Details of this matrix are shown in Figure 12. Note that

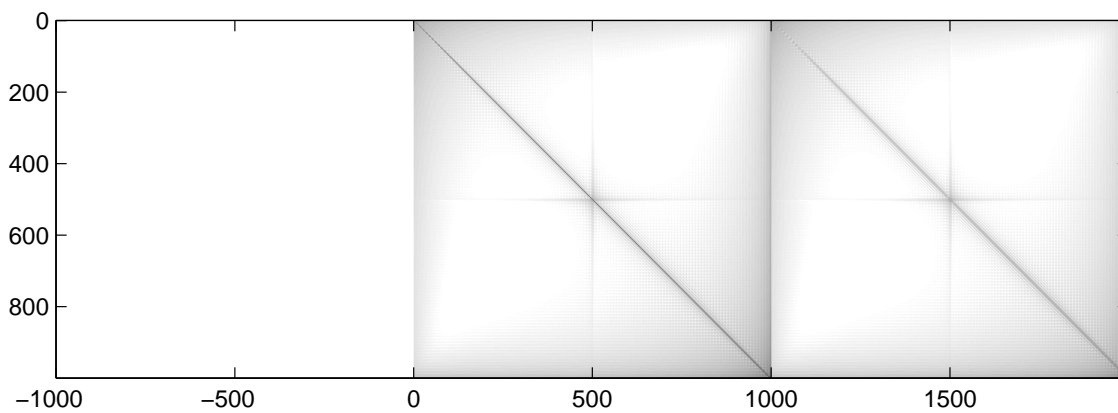


FIGURE 11. Channel matrix of a Weyl–Heisenberg family using a *cyclic prefix*.

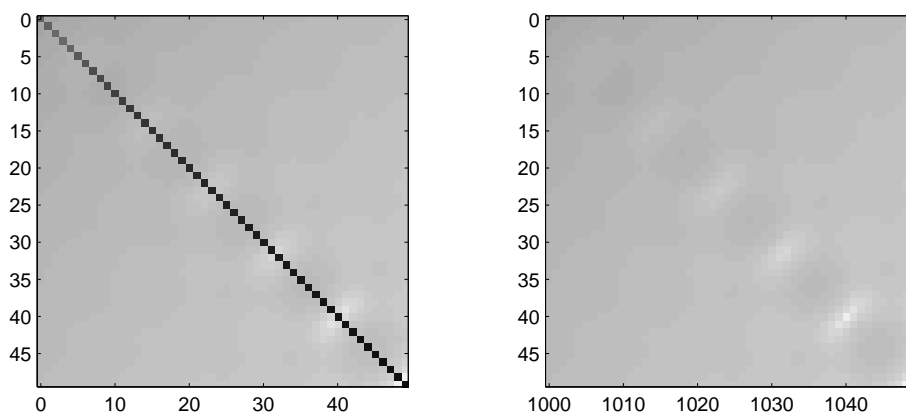


FIGURE 12. Details of Figure 11

we do not have exact diagonalization, since the duration of the *cyclic prefix* is smaller than the duration of the impulse response h (see Figure 6). Nevertheless, a significant improvement due to the *cyclic prefix* is obvious.

Remark. The real world requires real valued transmission signals. In the Weyl–Heisenberg case, not the complex valued function $f(x) = \sum_{k \in \mathbb{Z}} \sum_{l=1}^N c_{k,l} g_{k,l}$ is used to transmit information in form of the complex values $\{c_{k,l}\}_{l=1,\dots,N,k \in \mathbb{Z}}$ but the real valued signal $\tilde{f} = \frac{1}{2}(f + \bar{f})$. Nevertheless, an interference of \bar{f} on f only appears in the baseband and is negligible when using a window function with decent frequency localization.

4.2. **Wilson bases.** In analogy to the Weyl–Heisenberg bases of Section 4.1, we shall form a Wilson basis using $g_0(t) = \frac{1}{\sqrt{1000}} \chi_{[0,1000)}(t [\mu\text{s}])$ and $a = 1000\mu\text{s}$, $b = \frac{1}{1000}\text{MHz}$ and $M = 499$.

We order the elements according to

$$g_{n+4l+1997k} = g_{l,k}^{(n)}, \quad l = 1, \dots, 499, \quad k \in \mathbb{Z}$$

and

$$g_{1997k} = g_{0,k}, \quad k \in \mathbb{Z}.$$

A segment of the resulting channel matrix is displayed in Figure 13, and details can be seen in Figure 14.

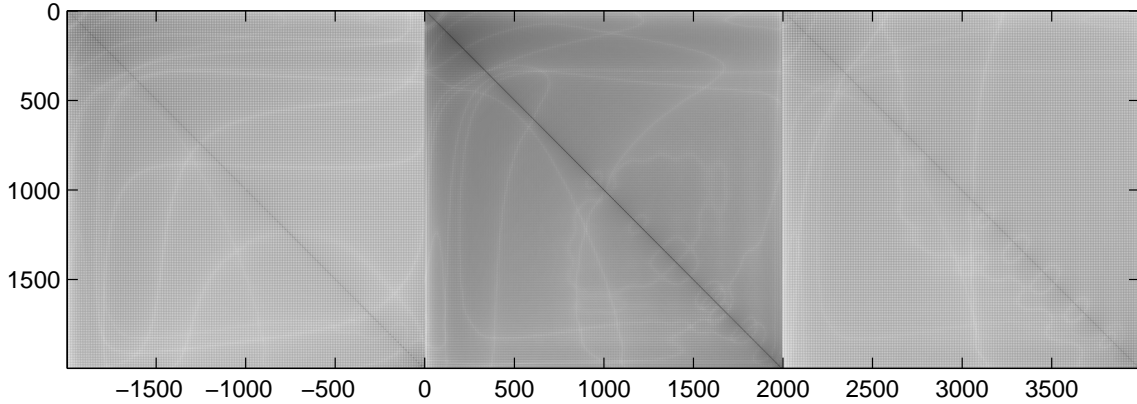


FIGURE 13. Channel matrix of a Wilson family.

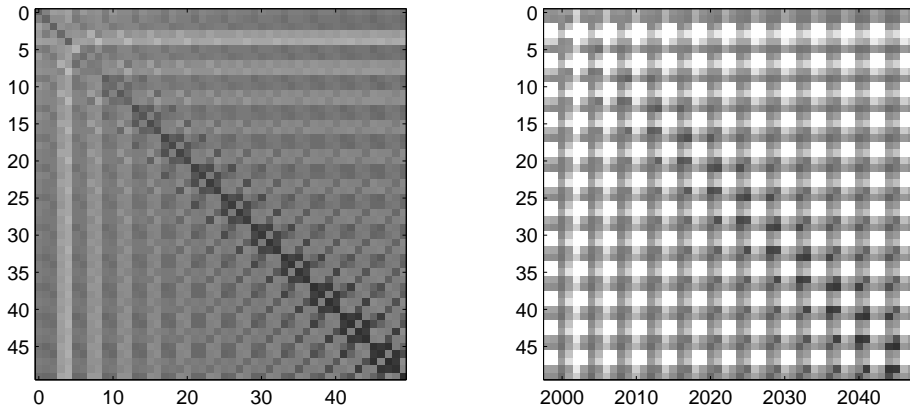


FIGURE 14. Details of Figure 13

4.3. **Wavelet bases.** To obtain an exemplary wavelet system we shall use the orthogonal Daubechies wavelet with 4 vanishing moments, i.e., $g_0 = \text{db4}$, scaled to support $[0, 7166]\mu\text{s}$ and normalized in the $L^2(\mathbb{R})$ sense. Furthermore, we set $a = 2^{10} = 1024\mu\text{s}$ and $M = 10$ and obtain the transmission family $\{g_{k,m}^{(n)}\}_{m=0,1,2,3,\dots,10, n=0,1,\dots,2^m-1, k \in \mathbb{Z}}$. The prototype function g_0 is displayed in Figure 15. Figure 16 shows the real and the imaginary part of the Fourier transform of $g_0 = \text{db4}$, i.e., $\text{Re}(\widehat{g}_0)$ and $\text{Im}(\widehat{g}_0)$.

We reorder the orthonormal wavelet family according to

$$g_{2047k+2^m-1+n} = g_{k,m}^{(n)}.$$

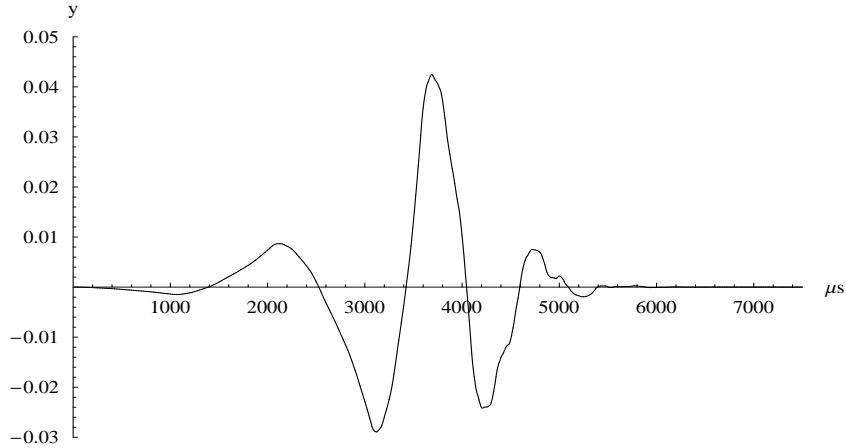


FIGURE 15. g_0 in the wavelet basis.

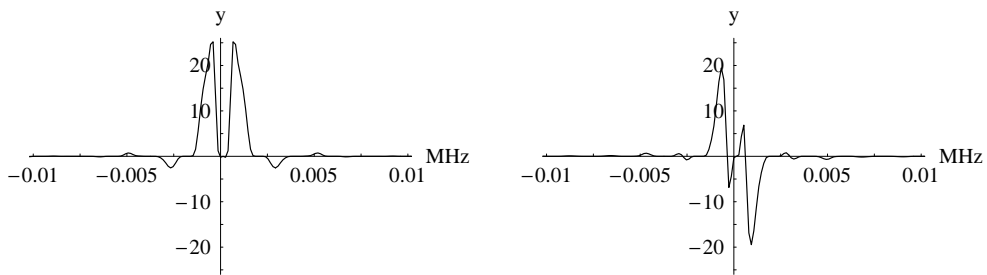


FIGURE 16. Real and imaginary part of the Fourier transform of g_0 .

A segment of the resulting channel matrix is displayed with logarithmic scale in Figure 17. The wavelet basis elements of the finest scale experience the strongest orthogonal perturbation, reflecting their poor frequency localization.

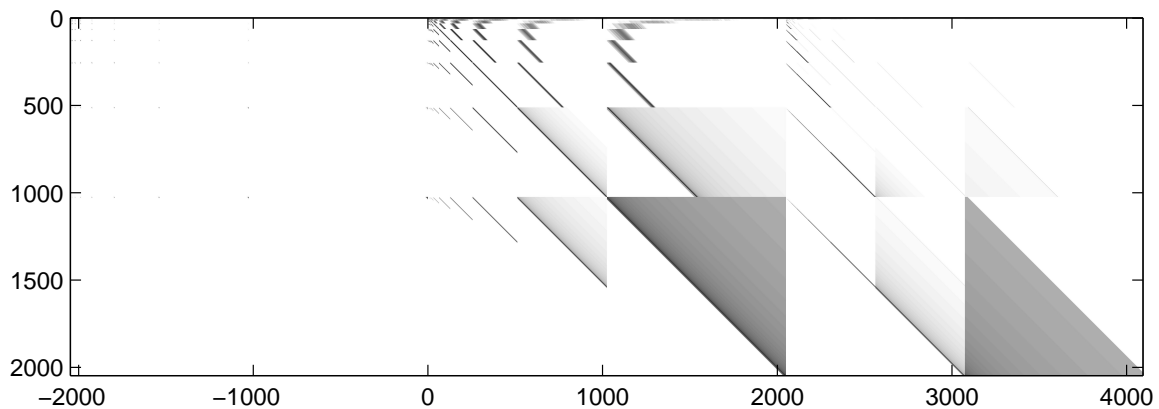


FIGURE 17. Channel matrix of a wavelet family.

CONCLUSION

We have shown that among the prominent coherent function systems we discussed (Gabor bases, Wilson bases, and wavelets), the Gabor bases are best matched to a set of convolution operators with practical importance.

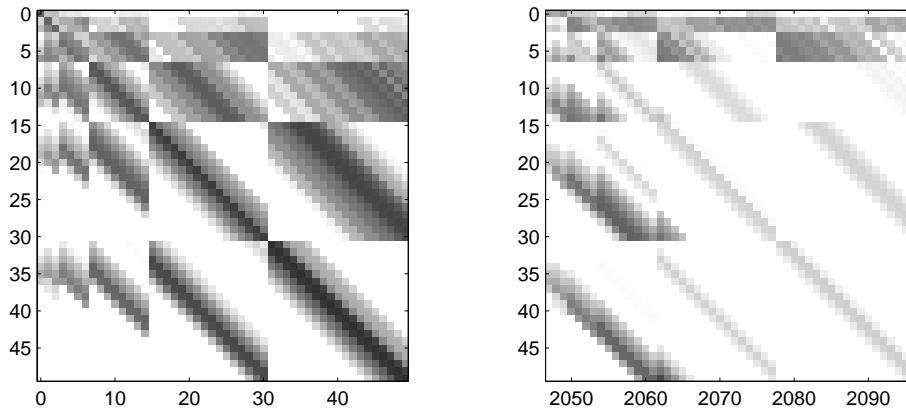


FIGURE 18. Details of Figure 17

Based on this result, the remaining open questions concern the design of Weyl–Heisenberg structured bases, i.e., finding the most bandwidth efficient tradeoff between frequency localization achieved through pulse shaping and inclusion of a *cyclic prefix* of a certain length.

ACKNOWLEDGEMENTS

The authors would like to express their thanks to K. Jetter for fruitful conversations and constructive comments.

Also, sponsoring by the German Ministry of Education and Science (BMBF) within the KOMNET program under grant 01 BP 902 is gratefully acknowledged.

REFERENCES

- [1] H. BÖLCSKEI, P. DUHAMEL and R. HLEISS, Design of pulse shaping OFDM/OQAM systems for high data-rate transmission over wireless channels. In: *Proc. of IEEE Int. Conf. on Communications (ICC)*, Vancouver 1999, pp. 559–564.
- [2] G. CHERUBINI, E. ELEFThERIOU, S. OELCER, and J. M. CIOFFI, Filter bank modulation techniques for very high speed digital subscriber lines. *IEEE Communications Magazine* May 2000, pp. 98–104.
- [3] I. DAUBECHIES, *Ten Lectures on Wavelets* CBMS-NSF Lecture Notes Nr. **61**, SIAM (1992).
- [4] I. DAUBECHIES, S. JAFFARD, and J. JOURNÉ, A simple Wilson orthonormal basis with exponential decay. *SIAM J. Math. Anal.* **22** No.2 (1991), pp. 554–572.
- [5] D.L. DONOHO and P.B. STARK, Uncertainty principles and signal recovery. *SIAM J. Appl. Math.* **49** (1989), pp. 906–931.
- [6] EUROPEAN TELECOMMUNICATIONS STANDARDS INSTITUTE, Transmission and Multiplexing (TM); Asymmetric Digital Subscriber Line (ADSL); Requirements and performance, ETSI ETR **328** ed.1 (1996)
- [7] C. FLAMMER, *Spheroidal wave functions*, Stanford University Press, Stanford 1957.
- [8] W. KOZEK and A.F. MOLISCH, Nonorthogonal pulseshapes for multicarrier communications in doubly dispersive channels. *IEEE J. Selected Areas in Communications* **16** (1998), pp. 1579–1589.
- [9] D. SLEPIAN and H.O. POLLAK, Prolate spheroidal wave functions, Fourier analysis and uncertainty — I. *Bell Syst. Tech. J.* **40** (1961), pp. 43–63.
- [10] H.J. LANDAU and H.O. POLLAK, Prolate spheroidal wave functions, Fourier analysis and uncertainty — II. *Bell Syst. Tech. J.* **40** (1961), pp. 65–84.
- [11] H.J. LANDAU and H.O. POLLAK, Prolate spheroidal wave functions, Fourier analysis and uncertainty — III: the dimension of the space of essentially time- and band-limited signals. *Bell Syst. Tech. J.* **41** (1962), pp. 1295–1336.
- [12] D.G. MESTDAGH, M.R. ISAKSSON and P. ODLING, Zipper VDSL: a solution for robust duplex communication over telephone lines. *IEEE Communications Magazine* **38** (2000), pp. 90–96.

- [13] G. WORNELL, Emerging applications of multirate signal processing and wavelets in digital communications. *IEEE Proc.* **84** (1996), pp. 586–603.
- [14] A. ZYGMUND, *Trigonometric Series I & II*, Cambridge University Press, Cambridge 1968.